Fatigue Damage Characterization of Non-crimp Fabric Reinforced Reactive Thermoplastic Composites at Room and Low Temperatures

Erli Shi, John Montesano

Composites Research Group,
Department of Mechanical & Mechatronics Engineering,
University of Waterloo, Canada

ICCM 2023

Contents

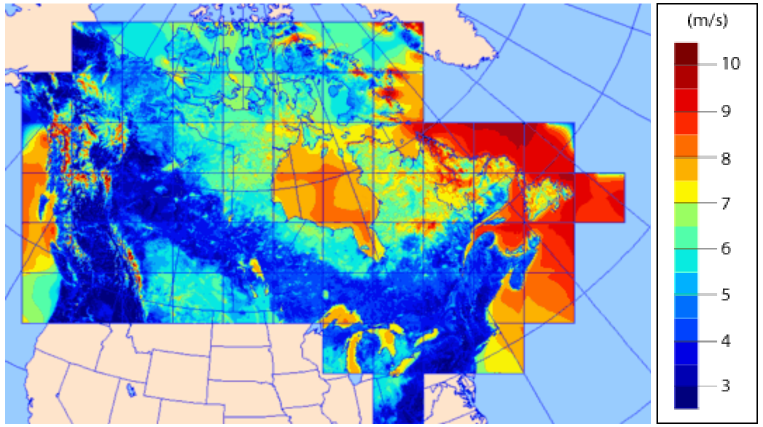

Overview of mean wind speed at 30m on Canadian territory [1]

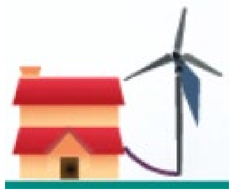

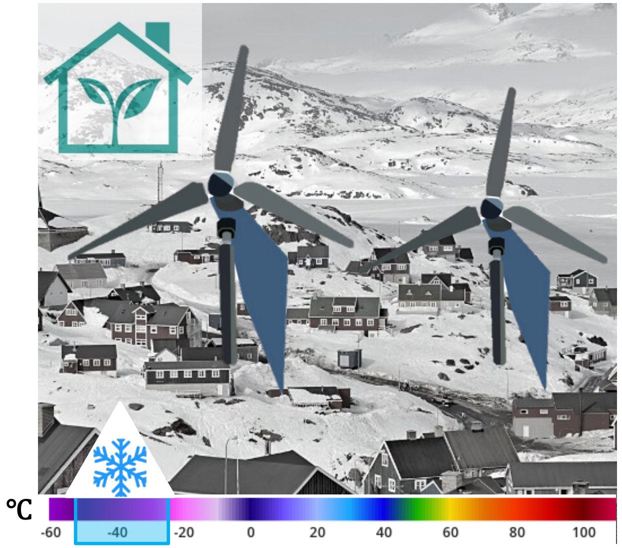

Shell and spar made of glass fiber/epoxy or carbon fiber/epoxy laminates

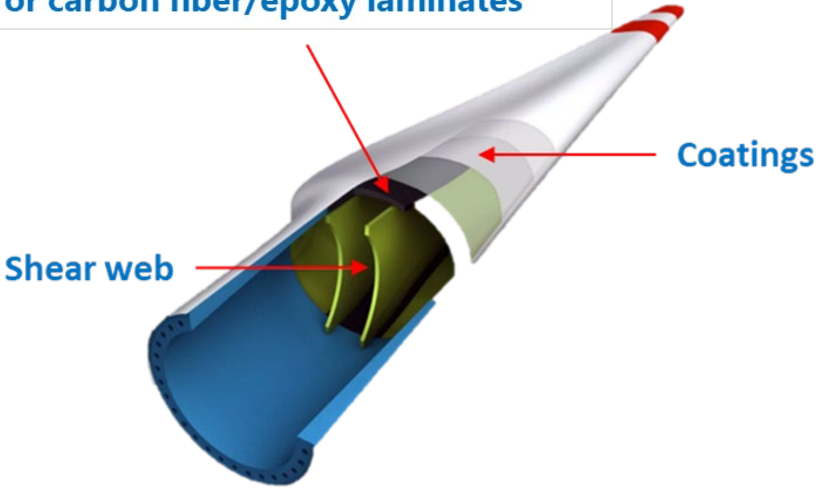

Traditional wind turbine blade structure

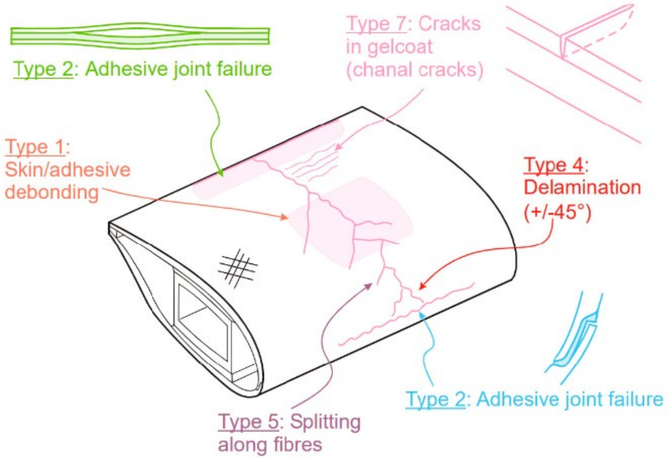

Typical failure modes of wind turbine blades [2]

Brittle failure mode of FRP composites at low temperature

Characterization of FRP composites at low temperatures:

Author	Test condition	Main findings
Gong et al. [3]	Static tension UD Glass / epoxy RT and -196.15°C (77K)	The ultimate tensile strength, Young's modulus, and strain at failure increased at 77K.
Torabizadeh et al. [4]	Static tension, compression, shear UD Glass / epoxy RT, -20°C, -60°C	The strength and modulus both increased with decreasing temperature in all cases, while the strain at failure decreased.
Cormier et al. [5]	T-T fatigue tests with R=0.1 NCF Glass / epoxy RT and -40°C	The fatigue life improved significantly at lower temperature, with a steeper decrease of the S-N curves.
Shindo et al. [6]	T-T fatigue tests with R=0.1 Woven Glass / epoxy RT, -196.15°C and -269.15°C (4K)	The fatigue life increased at 77K compared to RT, followed by significant loss when further decreasing the temperature to 4K.
Bureau et al. [7]	T-T fatigue tests with R=0.1 Woven Glass / PP RT and -40°C	GF/PP composites had excellent fatigue performance at RT, which improved at -40°C.

Research gaps:

- Few studies focus on characterizing the performance of fiber-reinforced composites at low temperatures
  - Most studies do not consider damage evolution and failure mechanisms
  - Fewer studies on fiber-reinforced thermoplastics

Opportunity – Fiber-reinforced reactive thermoplastics:

- May offer improved toughness and durability at low temperatures
- Compatible with current liquid resin infusion processes for wind turbine blades
- Recyclable

Resin infused glass fiber-reinforced reactive thermoplastic for wind turbine blades

Objective 1

Establish non-destructive damage monitoring techniques at RT and LT, e.g., optical, thermographic [8]

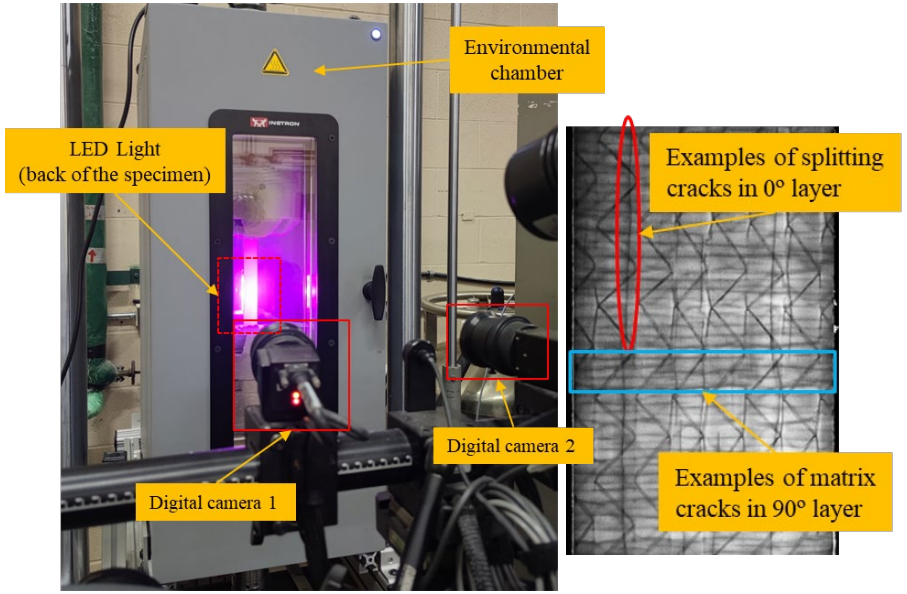

Objective 2

Characterize stress-strain response at RT and LT

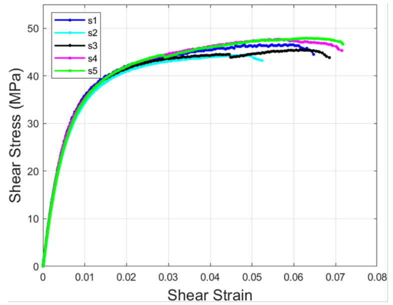

Stress-strain curve at RT

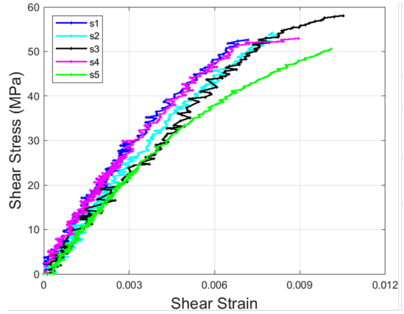

Stress-strain curve at -50°C

Objective 3

Study damage evolution and failure mechanisms under static and cyclic loading at RT and LT

--- New Optical Imaging Technique

--- Damage evolution, stiffness Degradation

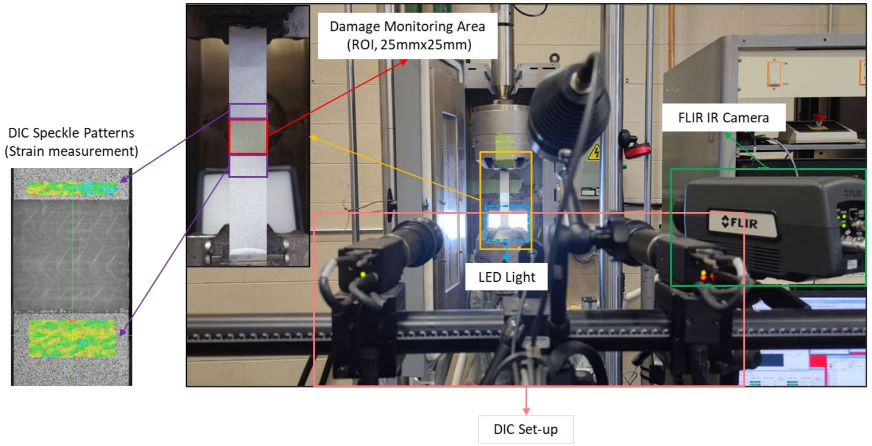

Front View

Material system: UD-NCF glass (Saertex ®) + Thermoplastic acrylic (Elium® 188 XO)

Fabric architecture:

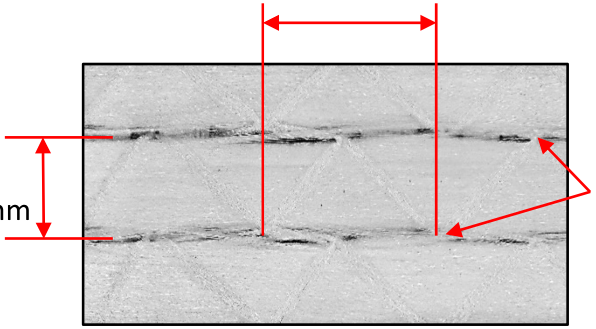

Top surface

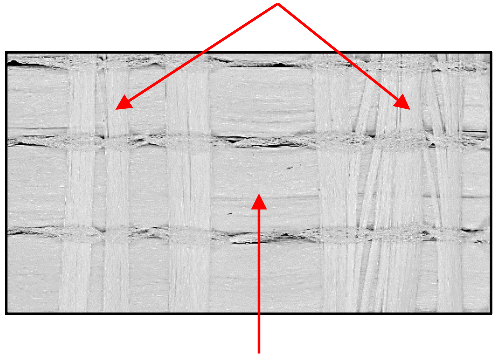

Bottom surface

Component	Orientation	Material	Areal density
Tow	0	E-glass 2400 tex	
Supporting Fibers	90	E-glass 275 tex	943 gsm
Stitching	Tricot pattern	Polyester 110 dtex	

Reactive thermoplastic acrylic resin:

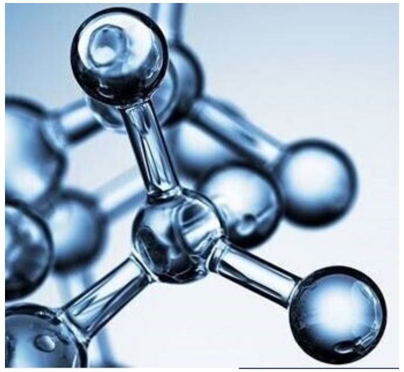

Resin properties:

Low viscosity: 0.1 Pa·s

Polymerization time at RT: 2 hours

Post-cure dry-Tg: 123°C

Recyclable, low density, high strength and toughness

Resin Infusion Process and Workflow

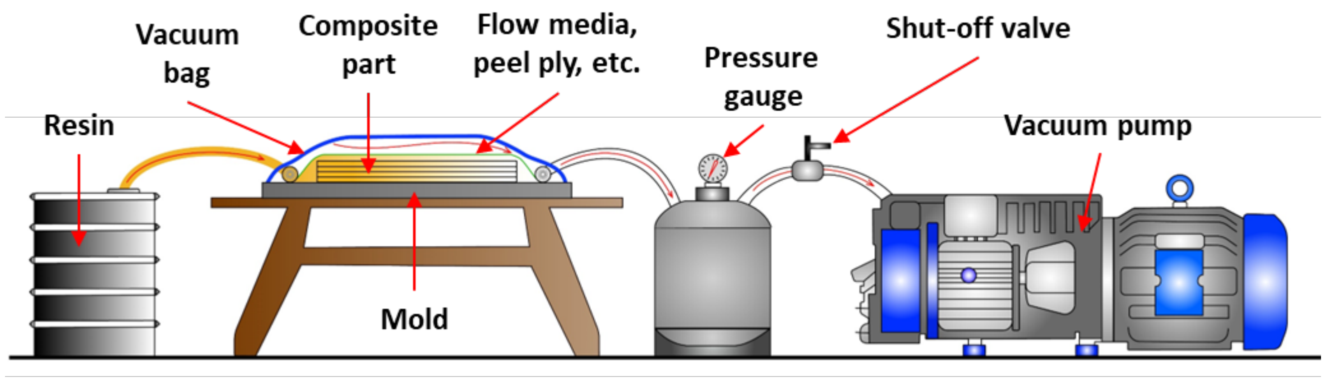

VARTM set-up

Panel mold side

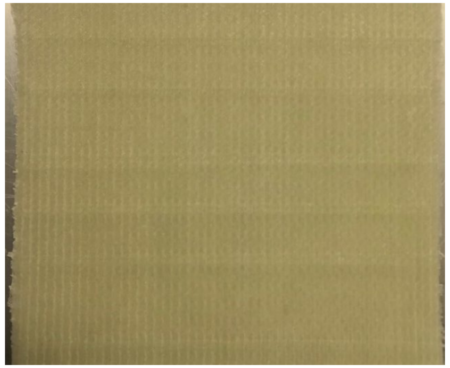

Panel vacuum bag side

Waterjet cutting machine

Test coupons

Mechanical test

Microscopic observation

Stacking sequence: $[0/90]_S$, V_f = 48%

Sample dimension: 275L x 25W x 2.8T
(Rectangular specimen for static tests; Dog bone specimen for fatigue tests)

Type of test:
Static tension: 2mm/min, ASTM D 3039
Tension-Tension fatigue: Peak stress 50%-75%UTS, R=0.1, 5Hz, ASTM D 3479

Test temperature: RT and -50°C

DIC Speckle Patterns
(Strain measurement)

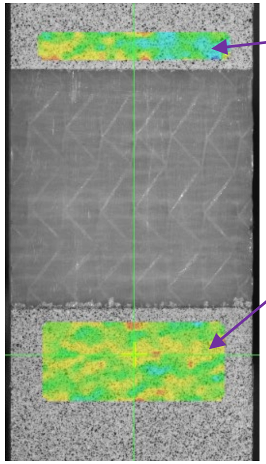

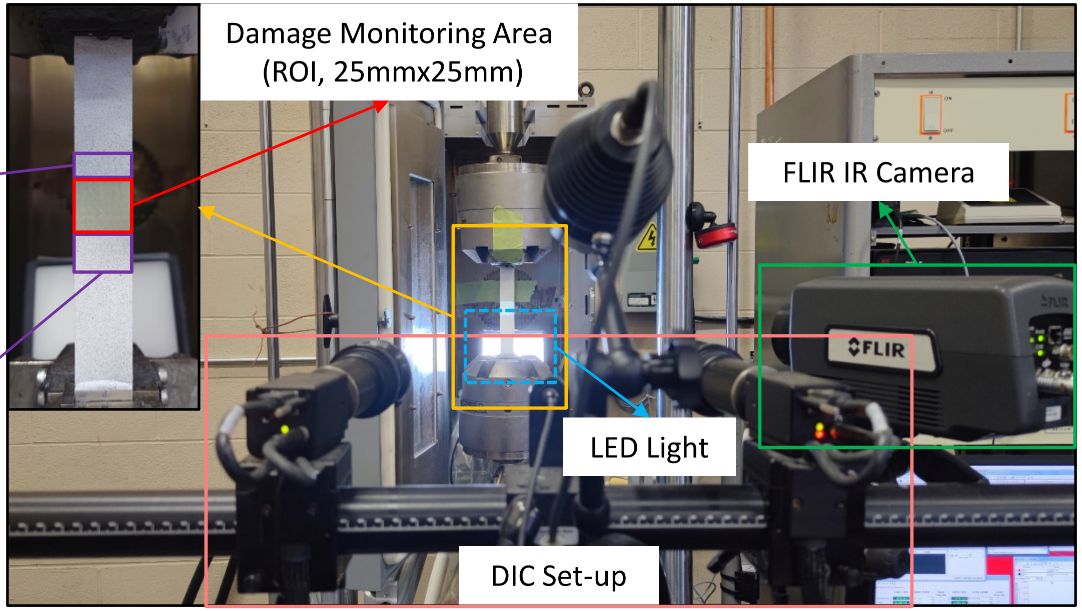

Test set-up for fatigue test

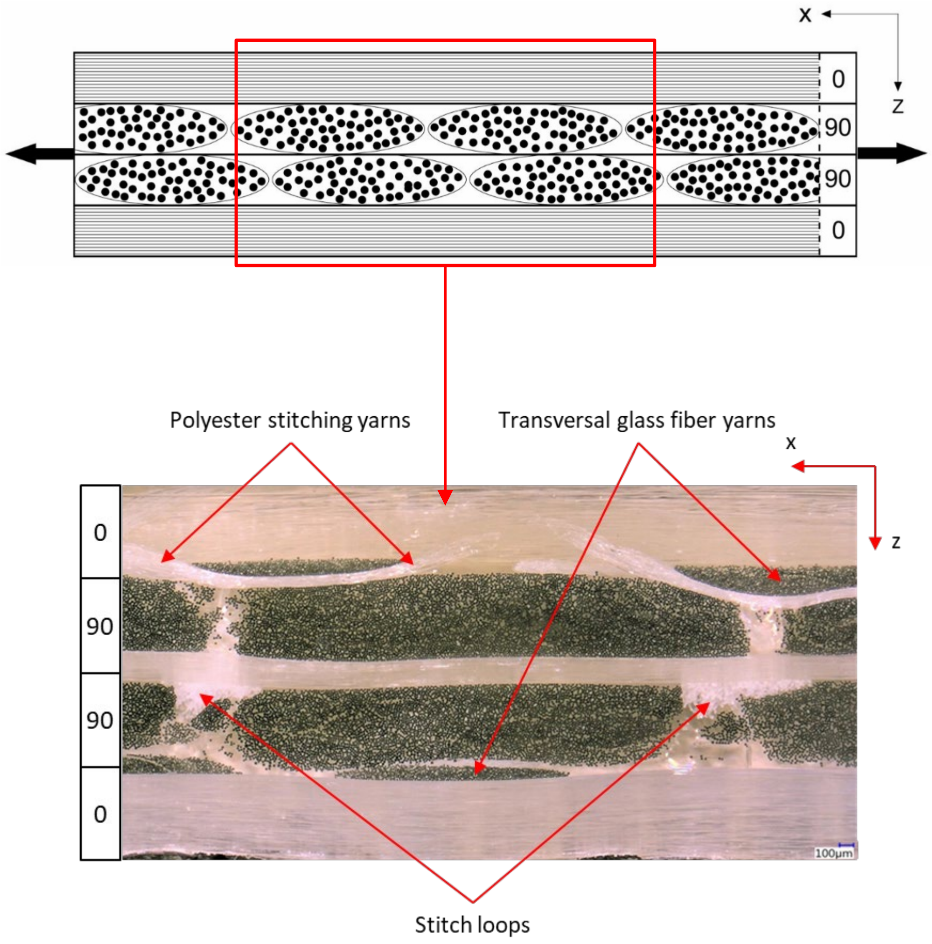

Stacking sequence

Quasi-static test results

5 quasi-static tests were conducted at each temperature condition.

Laminate properties				
	Tensile Strength (Mpa)	Modulus (GPa)	Strain at failure (%)	Strain at onset of failure (%)
RT	558.67 (±13.69)	24.69 (±0.42)	3.072 (±0.17)	~ 0.60
-50℃	582.21 (±22.46)	27.91 (±0.44)	3.144 (±0.26)	~ 0.26
Difference	+4.21%	+13.04%	+2.34%	-56.7%

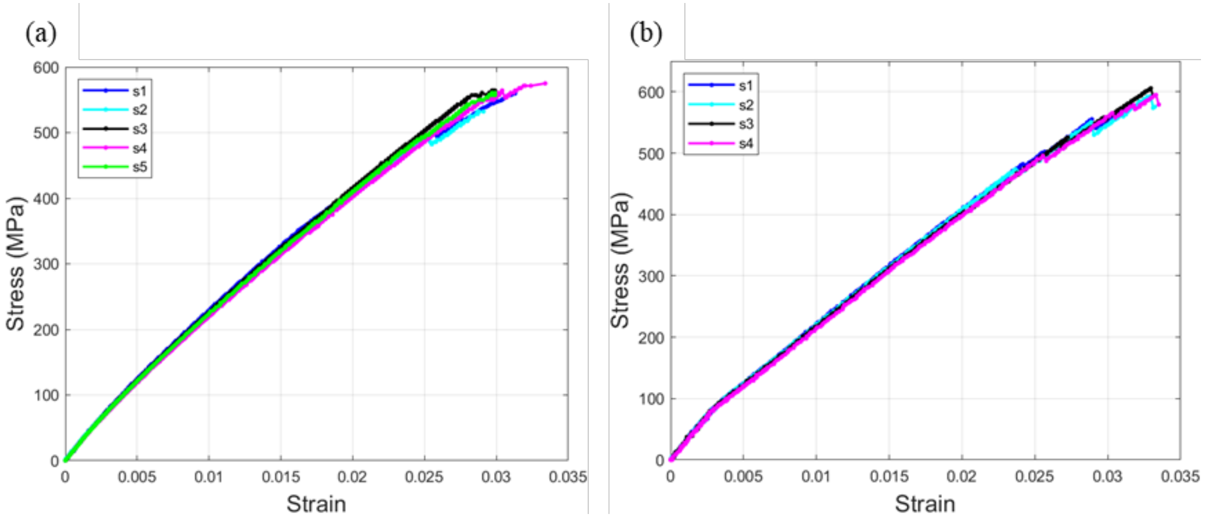

Laminate stress-strain response (a) RT, (b) -50°C

- A near linear stress-strain behavior **at RT**;
- An obvious bilinear stress-strain response **at -50℃** with a transition stress in the range of 12% -15% UTS (~ 0.26% strain).

Damage evolution of $[0/90]_s$ laminates at RT (Static)

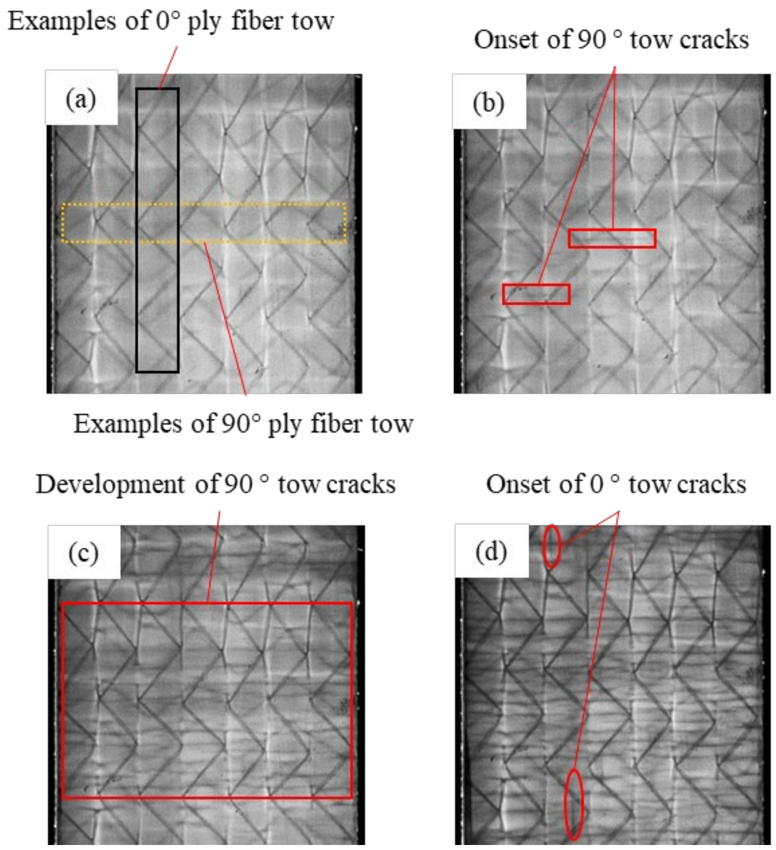

RT: (a) Undamaged stage, (b) 20% - 25% UTS, (c) 50% - 55% UTS, (d) 70% - 75% UTS.

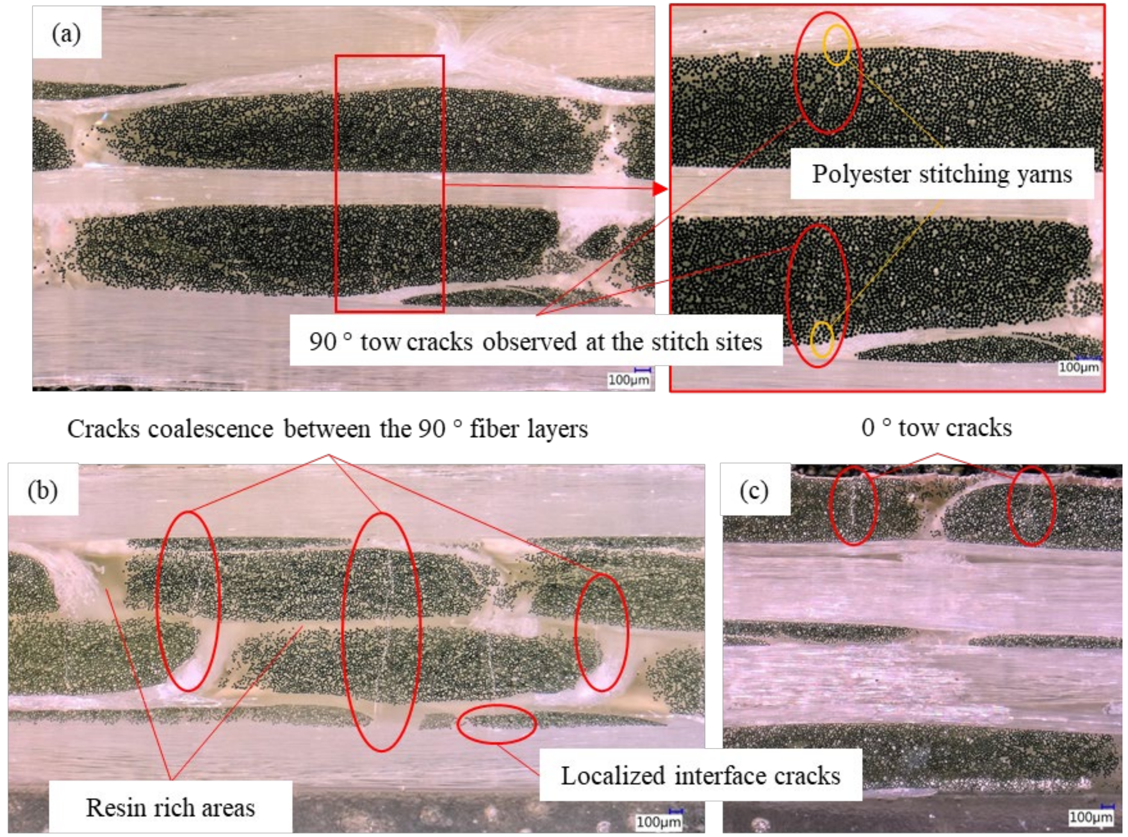

Microscopic observation of RT samples: (a) axial direction at 20%UTS, (b) axial direction at 70%-75%UTS, (c) cross-section direction at 70%-75%UTS.

Damage evolution of $[0/90]_s$ laminates at -50°C (Static)

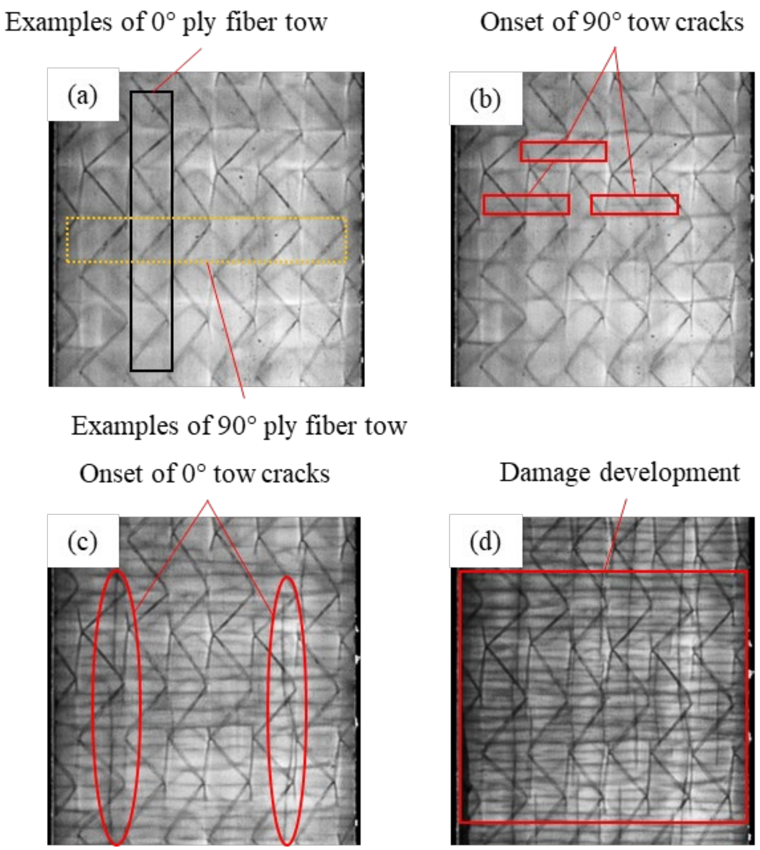

-50°C: (a) Undamaged stage, (b) 10% - 15% UTS, (c) 35% - 40% UTS, (d) 70% - 75% UTS.

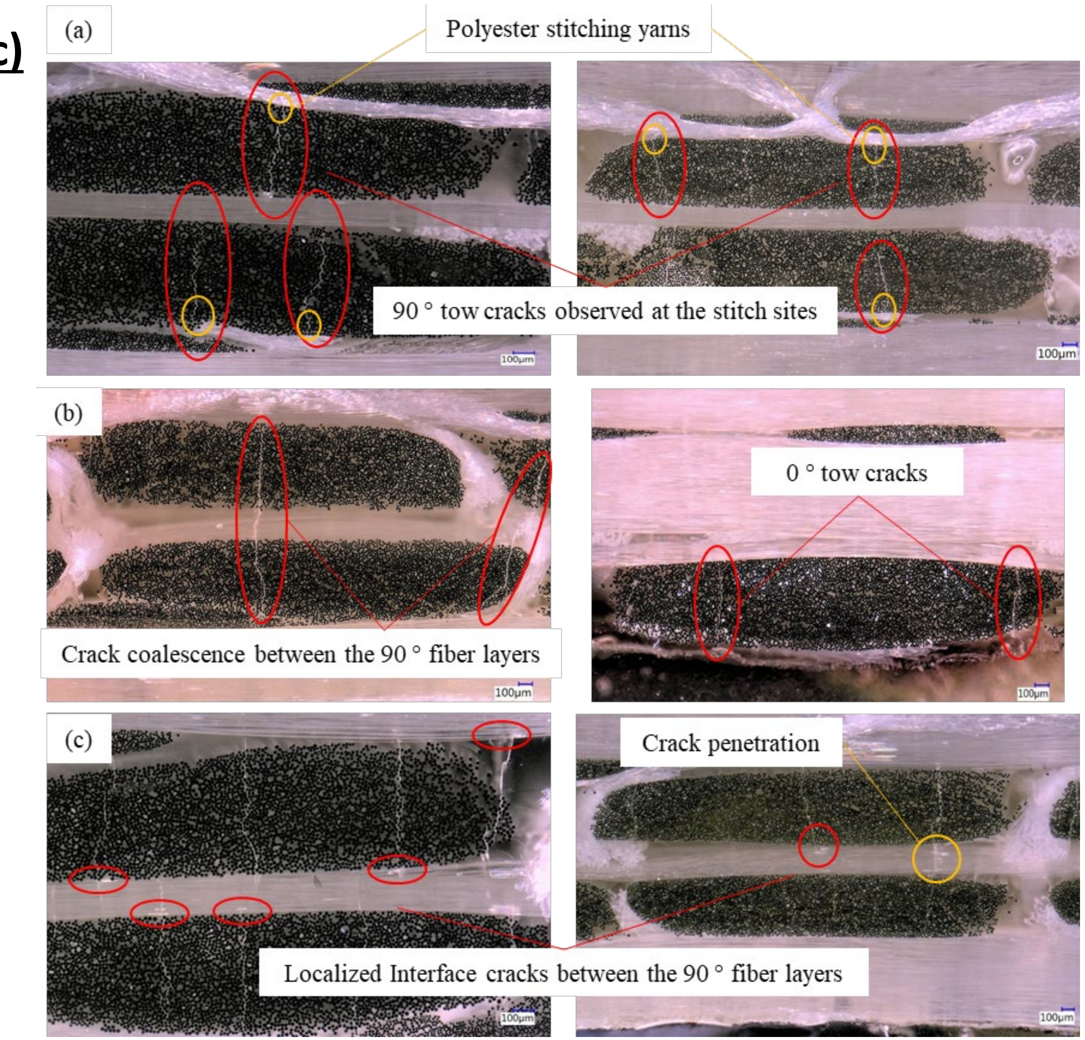

Microscopic observation of -50°C samples (a) axial direction at 20% UTS, (b) axial and cross-section direction at 50% UTS, (c) axial direction at 70%-75%UTS.

Fracture surface and damage evolution schematic (Static)

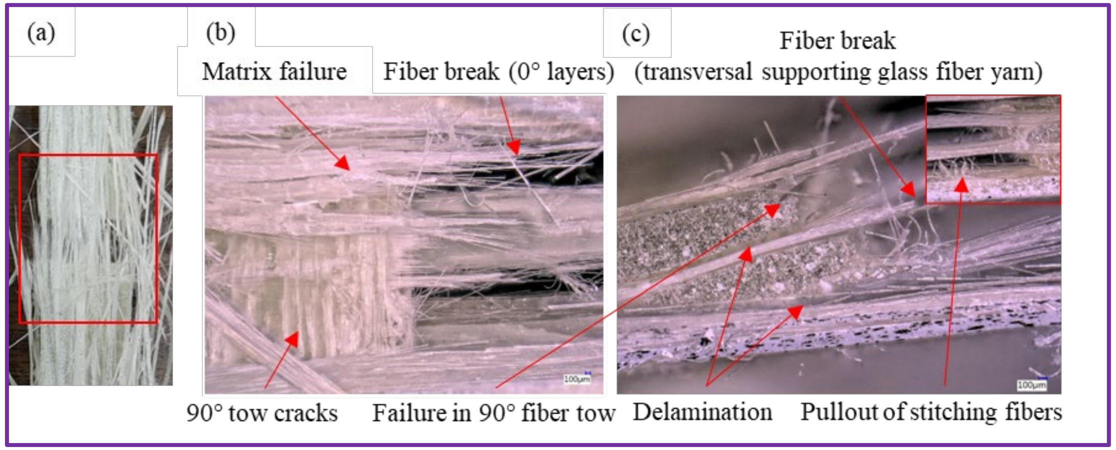

RT test specimen: (a) image of front fracture surface, (b) photomicrographs of front fracture surface, (c) photomicrographs of side fracture surface.

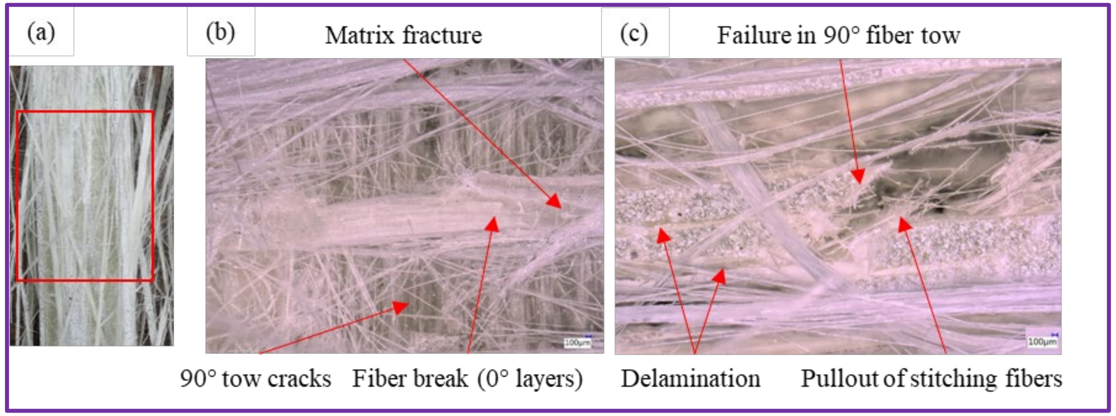

-50°C test specimen: (a) image of front fracture surface, (b) photomicrographs of front fracture surface, (c) photomicrographs of side fracture surface.

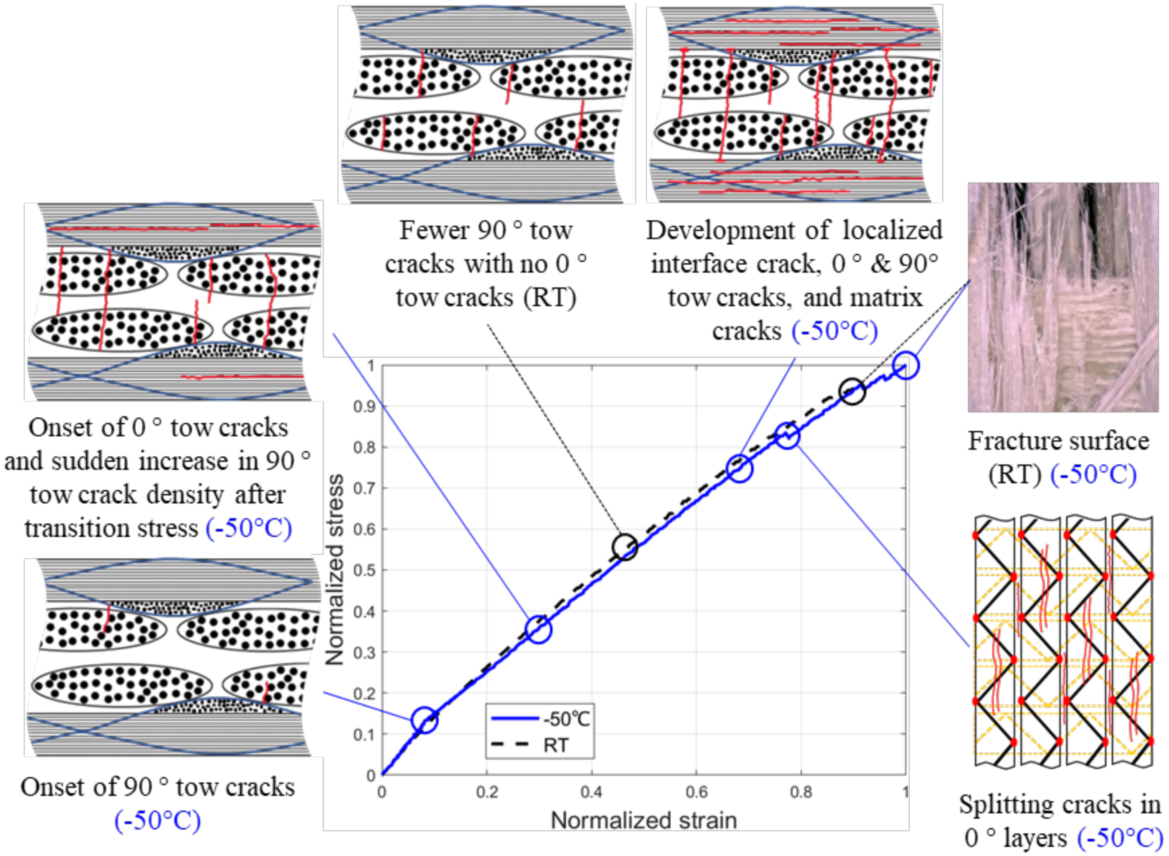

Schematic of damage evolution during static loading (only resin rich area between 90° fiber layers was shown)

Fatigue tests of $[0/90]_s$ laminates at -50℃ (preliminary)

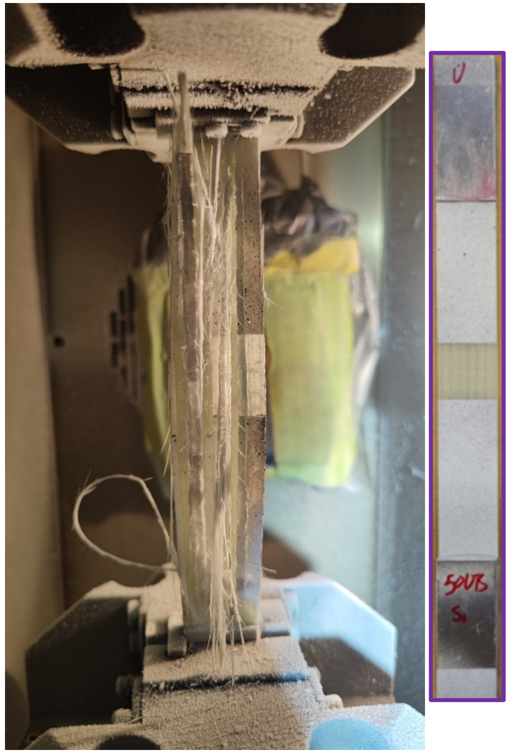

Rectangular specimen
(Failed at the end tab region)

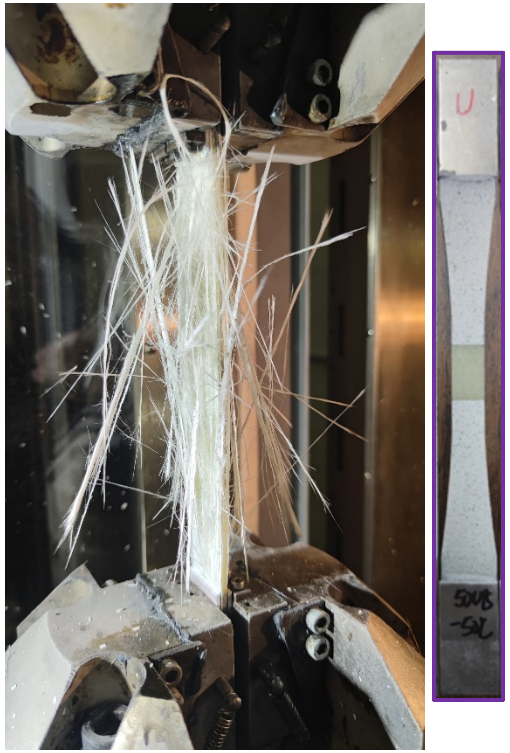

Dog bone specimen
(Failed at the gauge length region)

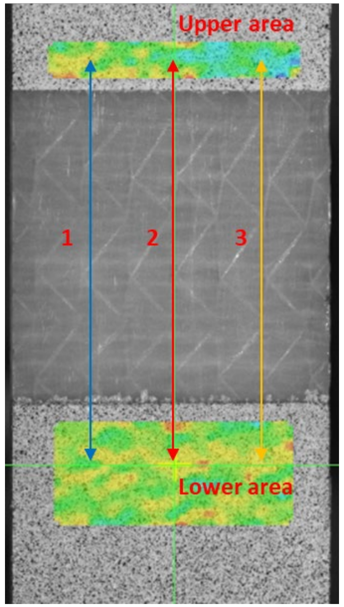

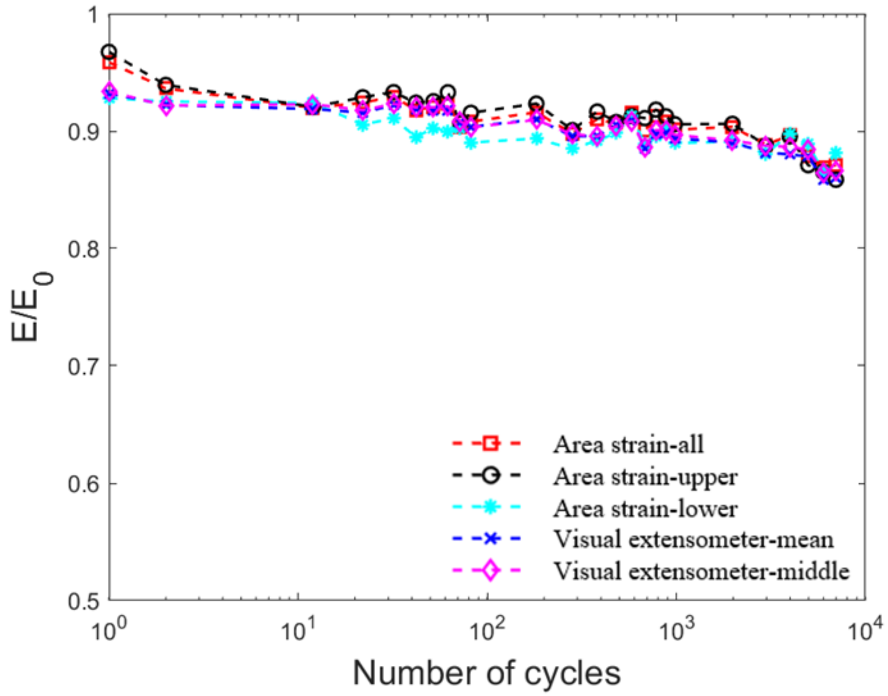

Stiffness degradation at room temperature (50% UTS)

Strain measurement schemes:
1: Averaged strain of all areas (upper area + lower area)
2: Averaged strain of the upper area
3: Averaged strain of the lower area
4: Averaged line strain of all visual extensometers (1 + 2 + 3)
5: Line strain of the middle visual extensometer (2)

Damage development at RT (Fatigue, 75%UTS)

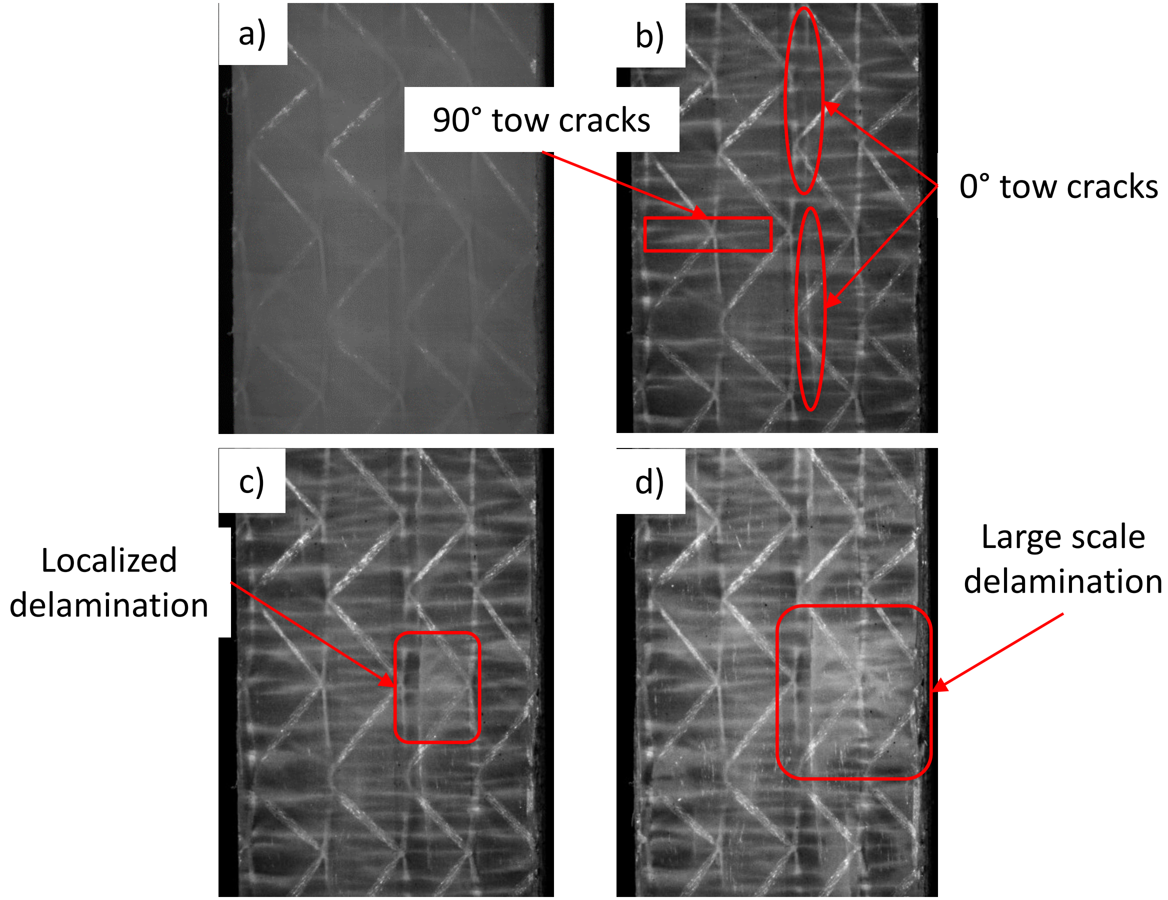

RT: (a) Undamaged stage, (b) 1st cycle, (c) 12% N_f, d) 97% N_f (N_f =875)

Damage development at -50℃ (Fatigue, 75%UTS)

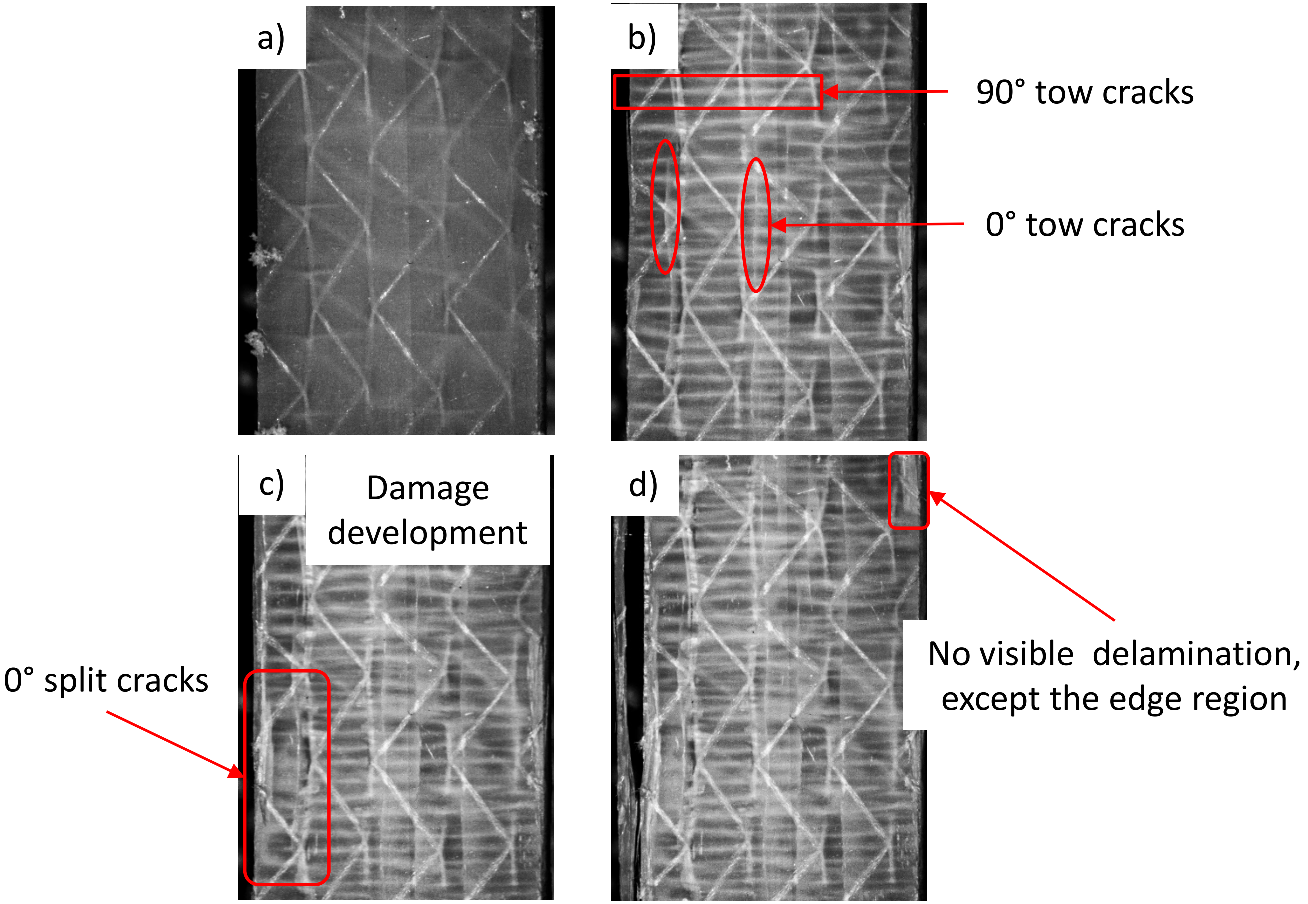

-50°C : (a) Undamaged stage, (b) 1st cycle, (c) 55% N_f, d) 91% N_f (N_f =1375)

1. The stress-strain response of UD-NCF glass fiber/acrylic composites at RT and -50°C is different (near linear vs obvious bilinear). However, similar damage modes were observed, i.e., 90° tow cracks, 0 ° tow cracks, matrix cracks, and interface cracks.
2. The ultimate tensile strength and Young's modulus increased at -50°C due to the increased resin strength and fiber-resin interface strength at low temperature.
3. At low temperature, damage tended to initiate at an early stage and was more advanced; however, there were fewer interactions between damage mechanisms causing stress relief and increased strain at failure.
4. For fatigue tests, the dog bone samples prevented premature failure, while the new strain measurement scheme enabled correlation of the damage evolution with stiffness degradation.
5. The damage development and failure mechanism of static tests and fatigue tests are different. The latter showed complicated damage modes at early stage (i.e., after 1 cycle). The damage evolution process at RT and -50°C is also different, and further validation is needed using microscope observation.

Future works:

1. Microscopic observations of failed specimens and interrupted specimens at different loading cycles to evaluate the failure mechanism and verify the observed damage modes at RT and -50 ℃;
2. Perform fatigue tests at different stress levels (40% UTS to 80% UTS) to extract S-N data;
3. Correlate the observed damage modes with stiffness degradation and evaluate the crack density evolution during cyclic loading.

Acknowledgements

Thank you to all sponsors for this project!

BORRUM ENERGY SOLUTIONS

SAERTEX®

OCI Where Next Happens

NSERC CRSNG

CSC SCHOLARSHIP A WAY TO YOUR DREAMS

ONTARIO Advanced Manufacturing Consortium

References

[1] The Wind Atlas, Environment and Climate Change Canada's Wind Atlas website, Environment and Climate Change Canada (RPN), accessed 2000, < http://www.windatlas.ca/index-en.php >.

[2] Abdul Ghani Olabi, Tabbi Wilberforce, Khaled Elsaid, Enas Taha Sayed, Tareq Salameh, Mohammad Ali Abdelkareem and Ahmad Baroutaji. “A Review on Failure Modes of Wind Turbine Component’’. Energies , 14(17), 5241, 2021.

[3] Gong M, Wang XF, Zhao JH. “Experimental study on mechanical behavior of laminates at low temperature”. Cryogenics 2007; 47:1–7.

[4] Torabizadeh MA. “Tensile, compressive and shear properties of unidirectional glass/epoxy composites subjected to mechanical loading and low temperature services”. Indian J Eng Mater Sci 2013;20:299–309.

[5] Laurent Cormier, Simon Joncas and Rogier P.L. Nijssen. “Effects of low temperature on the mechanical properties of glass fibre–epoxy composites: static tension, compression, R= 0.1 and R=-1 fatigue of $\pm 45^{\circ}$ laminates”. Wind Energy, Volume 19, pp 1023–1041, 2016.

[6] Yasuhide Shindo, Satoru Takano, Katsumi Horiguchi, Takashi Sato. “Cryogenic fatigue behavior of plain weave glass/epoxy composite laminates under tension–tension cycling”. Cryogenics, Volume 46, pp 794-798, 2006.

[7] M. N. BUREAU* and J. DENAULT. “Fatigue Resistance of Continuous Glass Fiber/Polypropylene Composites: Temperature Dependence’’. POLYMER COMPOSITES, Vol. 25, No. 6, DECEMBER 2004.

[8] Shi EL, Montesano J. “Fatigue Behavior of A Unidirectional Non-crimp Fabric Glass Fiber Reinforced Reactive Thermoplastic Composite," presented at the 12th Canadian-International Conference on Composites. 2022.

Thank You!